

Resistance Analysis of Remotely Operated Vehicle (ROV)

Rr. Niken Danartika Hadi Putri ^{1*}, I Ketut Suastika ¹.

¹Department of Naval Architecture, Institut Teknologi Sepuluh Nopember, Surabaya, Indonesia

Abstract. Indonesia's vast underwater resources and infrastructure necessitate advanced technologies for exploration and maintenance. Remotely Operated Vehicles (ROVs) have emerged as essential tools, offering safe and efficient underwater operations. However, their performance is affected by hydrodynamic drag, influencing maneuverability and energy efficiency. This study may differ from previous research due to the ROV model used. The TKD Laboratory UUV model, named Segara Nauta with the type code SN-01, is currently under development in the TKD Laboratory of the Department of Naval Architecture, Faculty of Marine Technology (FTK) – ITS is used for this study. This study is focused on investigating the drag characteristics of the SN-01 ROV using Computational Fluid Dynamics (CFD) simulations. Grid independence tests identified an optimal mesh resolution of 1,163,064 elements, balancing computational efficiency and accuracy. Resistance tests at varying speeds (0.3–1.0 m/s) and movement directions revealed that resistance increases with speed. Forward-backward resistance ranged from 0.0019 N to 0.0190 N, while sideways resistance was significantly higher, from 0.0049 N to 0.0481 N, due to greater surface exposure. The resistance on the ROV increases as the speed of the ROV increases, therefore it is necessary to conduct a study on the service speed of the ROV SN-01 because it can affect the selection of the engine used so that the ROV can work effectively and efficiently. These findings underscore the influence of motion direction and speed on hydrodynamic resistance, emphasizing the need for optimized ROV designs. The results provide valuable insights for improving ROV efficiency, supporting Indonesia's sustainable underwater exploration and maritime infrastructure maintenance.

1. Introduction

Indonesia boasts an abundant wealth of underwater natural resources, including oil, natural gas, and minerals such as gold, copper, nickel, and iron ore. As one of the largest oil and gas producers in Southeast Asia, the country exploits these resources in offshore waters and mineral-rich regions such as Papua, Maluku, Sulawesi, and Kalimantan. Additionally, other potential underwater resources, such as marine minerals, gas hydrates, and marine biomass, are currently under exploration and research.

As an archipelagic nation, Indonesia has extensive underwater installations, including oil and gas pipelines (subsea pipelines), subsea risers, PLEMs (Pipe Line End Manifolds), as well as subsea communication (fibre optic) and power cables. These infrastructures require regular monitoring and inspection to identify potential damage or disruptions, ensure safety, and maintain their technical functionality. The growing activities in seabed mining and the construction of underwater pipelines and cables have driven an increase in underwater observation activities, both for surveys and inspections. By using unmanned technology and systems on underwater marine vehicles, namely Autonomous Underwater Vehicles (AUV), the underwater observation process will be assisted and safer (Sahir et al., 2017).

Remotely Operated Vehicle (ROV) technology has emerged as a primary solution to address the risks and limitations of human diving, particularly at depths of 100–300 meters. The use of ROVs offers safer, more cost-effective operations and allows for broader reach compared to manual diving. ROVs are equipped with tools such as cameras, sonar, and various sensors to support data collection. Additionally, Autonomous Underwater Vehicles (AUVs) are being developed as an alternative unmanned technology for underwater monitoring, although the mastery of such technology remains limited in Indonesia.

However, the performance of ROVs is influenced by hydrodynamic drag, which affects their maneuver ability, maximum speed, and energy efficiency. Therefore, studying the hydrodynamic drag on ROVs is essential for optimizing their design to enhance performance in supporting underwater surveys and inspections, particularly for pipeline infrastructure. Optimizing ROV designs with a focus on drag reduction will provide more efficient and safer technological solutions, supporting Indonesia's underwater exploration activities in a self-reliant and sustainable manner.

Research on Resistance Analysis of Remotely Operated Vehicle (ROV) may differ from previous research due to the ROV model used. The TKD Laboratory UUV model, named Segara Nauta with the type code SN-01, is currently under development in the TKD Laboratory of the Department of Naval Architecture, Faculty of Marine Technology (FTK) – ITS.

*Corresponding author: rnikendanartika@gmail.com

Development of this model begins in 2023, focusing on design and electronics aspects as part of a final project (Ramadhani, 2023). This underwater vehicle features a fish-line body design, emphasizes hydrodynamic properties, and incorporates a modular structure.

2. Methodology

2.1. Remotely Operated Vehicle (ROV)

A Remotely Operated Underwater Vehicle (ROUV) is an underwater vehicle physically connected to an operator via a cable and controlled by an operator located on a vessel above the water surface (Gómez et al., 2017). This robot-like machine allows the operator to maneuver it from a relatively safe, dry, and comfortable location, typically on a ship or platform situated on the water's surface above the ROUV. The ROUV is classified as a tethered unmanned submersible robot. It is uninhabited, highly maneuverable, and operated by a human. The ROUV plays a critical role as an underwater robot, enabling operators to remain in a safe and comfortable environment while the ROUV performs tasks in hazardous underwater conditions (Azis et al., 2012).

2.2. ROV Model

The TKD Laboratory UUV model, named Segara Nauta with the type code SN-01, is currently under development in the TKD Laboratory of the Department of Naval Architecture, Faculty of Marine Technology (FTK) – ITS. Development of this model began in 2023, focusing on design and electronics aspects as part of a final project (Ramadhani, 2023). This underwater vehicle features a fish-line body design, emphasizing hydrodynamic properties, and incorporates a modular structure as shown in Figure 2.

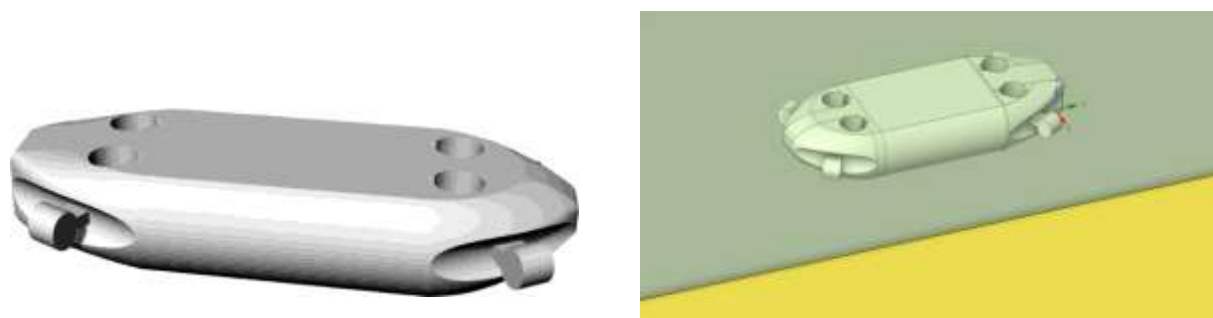


Figure 1 ROV Model

The modeling of the UUV SN-01 consists of components divided into the front, rear, and middle body sections, along with a thruster. Modifications were made to the components to simplify certain parts of the model for the meshing process. This simplification aims to reduce the geometric complexity of the model and minimize the size of the elements used to construct the geometry. The ROV model geometry specifications as a model are described in Table 1.

Table 1 Principal Dimension

Principal Dimension		
Length Overall	4,356	m
Bow length	1,016	m
PMB length	2,229	m
Aft length	1,111	m
Diameter	0,508	m
Wetted Surface Area	5,989	m ²
CG from bow	2,009	m

2.3. Computational Fluid Dynamics (CFD)

Computational Fluid Dynamics (CFD) is a field in science that, with the assistance of computers, provides quantitative predictions of fluid flow based on conservation laws (conservation of mass, momentum, and energy). CFD predictions refer to the defined flow geometry, physical properties, as well as boundary and initial conditions. The CFD computation principle begins by dividing the fluid domain into several integrated elements. Each element is governed by an equation using numerical calculations, which then produce results such as forces acting on the model or other information that describes the model's condition under specific boundary conditions. These boundary conditions are required as input. This principle is commonly employed in computational calculations using computer assistance. Another

example of the application of this principle is Finite Element Analysis (FEA), which is used to calculate stress occurring in solid objects. (Kundu & Cohen, 2012).

2.4. Variation Determination

The test parameters in the CFD analysis of this study include control variables, constant variables, and free variables. The control variables consist of the operational speed and depth of the ROV, the constant variables include the speed and angles of the fluid inlet and outlet, while the free variables include the characteristics of the fluid flow passing through the ROV. The model was tested at 6 Speed Variations on Forward-Backward movement and 6 Speed Variations on Left-Right movement. As shown in Table 2.

Table 2 Variation Determination

No.	Forward - Backward	Right - Left
	Speed (m/s)	Speed (m/s)
1	0,3	0,3
2	0,4	0,4
3	0,55	0,55
4	0,6	0,6
5	0,7	0,7
6	1	1

2.5. Computational Domain, Boundary Conditions and Meshing

The simulation domain is established to represent the flow in the area around the model and is solved using numerical methods. Choosing the simulation domain is vital in demonstrating how the model's shape impacts the flow passing through it. The domain setup follows the guidelines recommended by the ITTC regarding the placement of the model in relation to the domain boundaries. This is important to ensure that the boundaries of the domain do not affect the flow around the model. The minimum distance between the domain boundaries and the model should be at least 1-2 times the length between perpendiculars (Lpp) (ITTC, 2011).

As seen in Figure 3, the computational domain is shaped like a box, with the boundaries located as follows. As seen in Figure 3, the computational domain is shaped like a box, with the boundaries located as follows. The outflow is situated 4000 downstream from the vessel, and the entry is situated 2000 upstream. The side walls are about 2000 feet away from the ship. The top wall is 2000 feet above the vessel, while the bottom wall is 2000 feet below it. In order to adequately capture the contour of the wave pattern behind the vessel, the domain length was made rather long (4000).

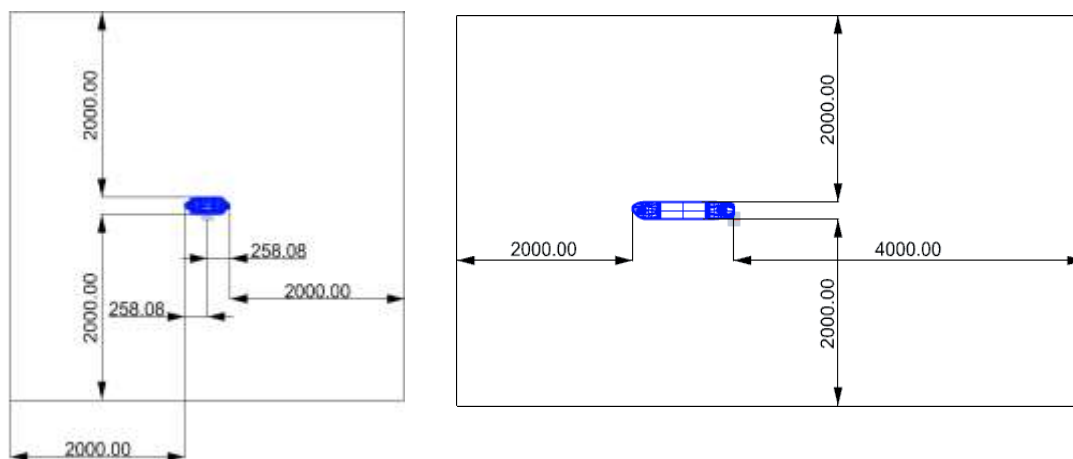


Figure 2 Ship Domain

Accurately depicting the fluid flow along the ship hull that is, the boundary layer flow that influences the vessel's drag is crucial. As a result, the mesh close to the hull was improved. In order to capture the free surface effects that is, the waves produced by the movement of the vessel on the water's surface the mesh close to the free surface was further improved. A side view of the computational mesh, using a multi-block structured grid, is displayed in Figure 4, with mesh improvements in the areas close to the hull and the free surface.

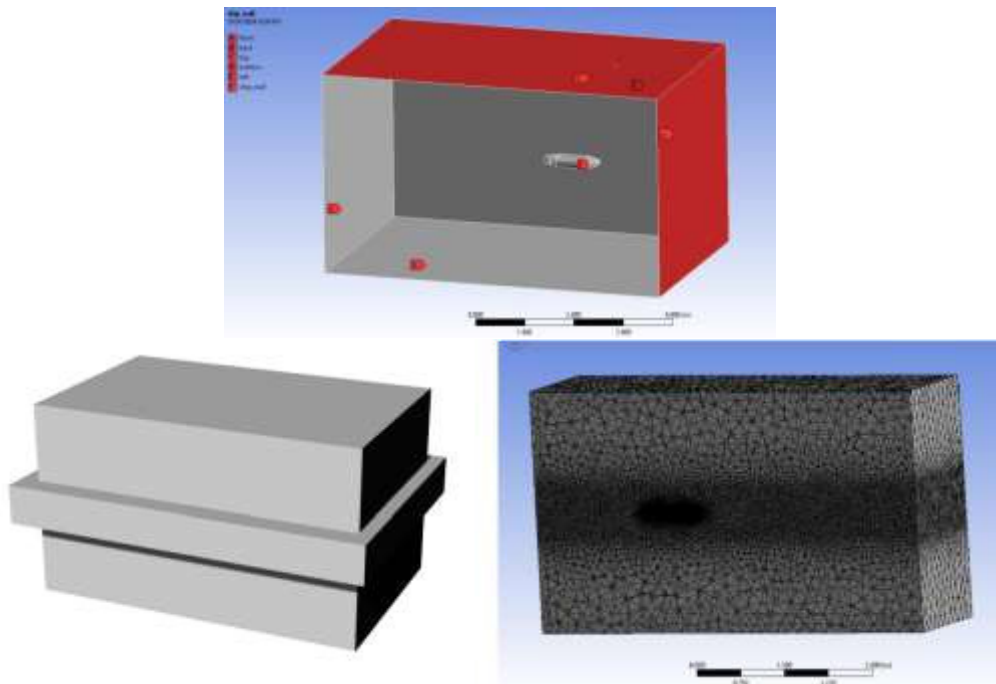


Figure 3 3D Side view of the computational mesh

2.6. Grid Independence Tests

To ascertain the ideal number of cells to be employed in the final setup of the CFD simulations and to confirm the convergence of the numerical computations, grid independence tests were conducted. The percentage rise or decrease in total resistance derived from these two consecutive simulations was calculated. In these experiments, the number of cells in a succeeding simulation was raised roughly 1.5 times until twice from the previous one. Table 3 tabulates the results, and plotted in Figure 5.

Table 3 Table Ship Resistance

Elements Qty.	Max Pressure (Pa)	Deviation	Ship Resistance (N)	Deviation
222855	0,05397		0,002013891	
568157	0,05401	0,07%	0,001969126	-2,22%
1163064	0,05294	-1,98%	0,001889085	-4,06%
2363086	0,05379	1,61%	0,001858333	-1,63%

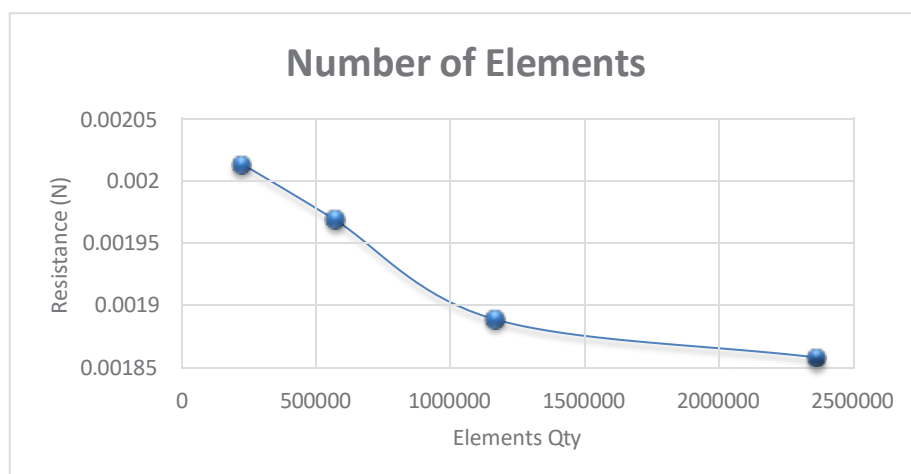


Figure 4 Result of Grid Independence Tests

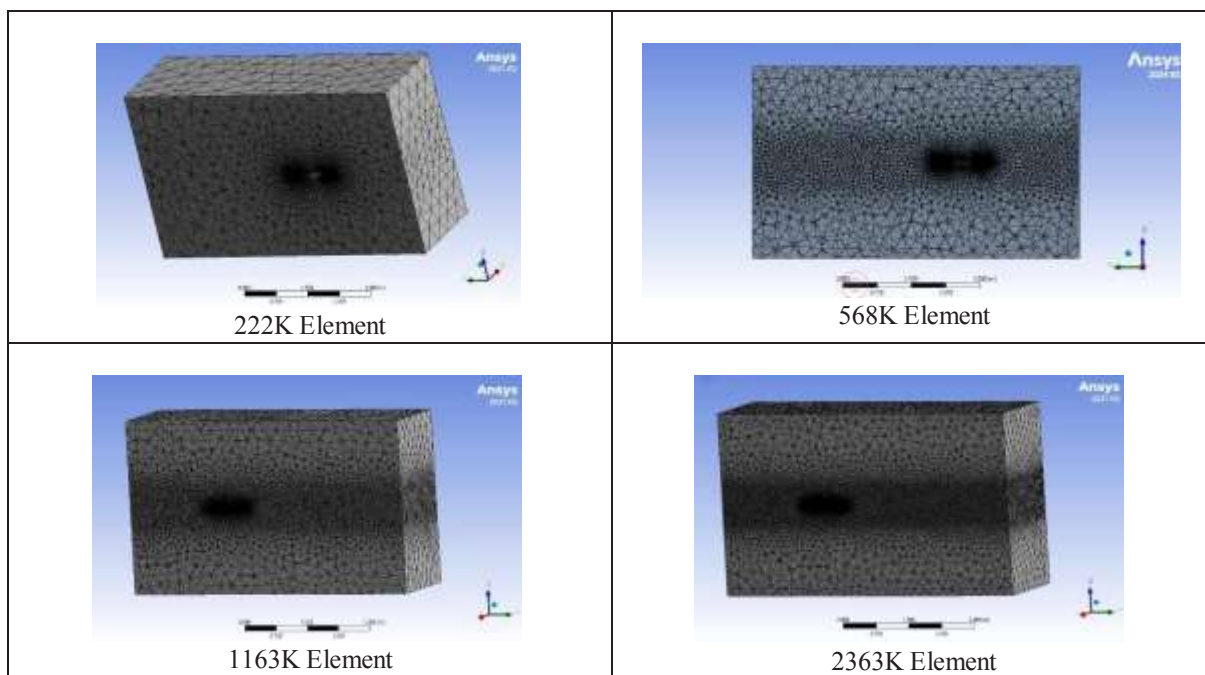


Figure 5 Meshing Trial Results at 0.3 m/s velocity.

From Table 3, the Deviation result with the most stable value is obtained, which is in the third row of the table or written in Table 4.

3. Results and Discussion

When the Deviation has been found, the next step is to look for Resistance in each Variation that has been determined. The table below is the result of Resistance in the Forward-Backward Variation. The results of the variation experiments carried out with the CFD method are Resistance which continues to grow along with the increasing speed on the ship both on the ship with the forward state and the ship in reverse state, as seen in Figure 6 and Table 4. When the ship is traveling at a speed of 0.3 m/s, the resistance is 0.0019 N until the ship increases the speed to 1.0 m/s, the resistance is 0.0190 N.

Table 4 Result of Resistance in the Forward-Backward

No	Speed (m/s)	Resistance (N)	
		Front - Back	Back - Front
1	0,30	0,001858333	0,001872720
2	0,40	0,003233097	0,003251852
3	0,55	0,005967690	0,006010472
4	0,60	0,007057926	0,007106079
5	0,70	0,009468552	0,009663272
6	1,00	0,019024893	0,019099682

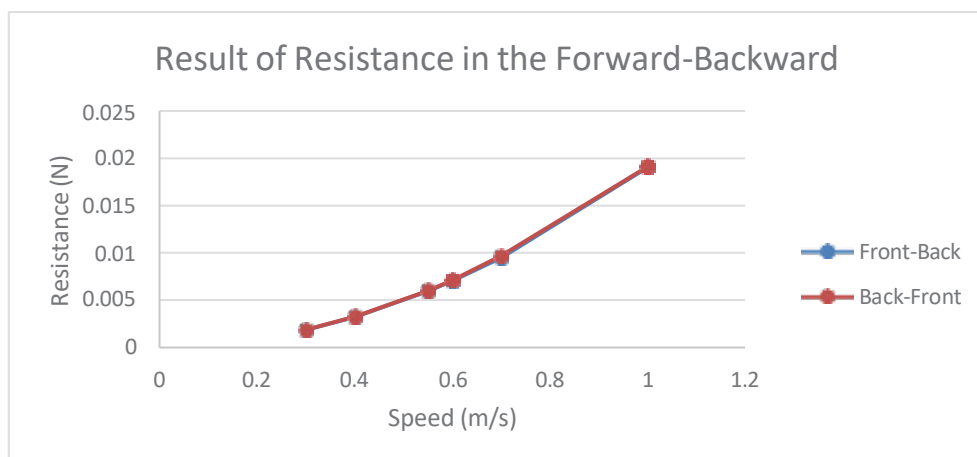


Figure 6 Diagram Result of Resistance in the Forward-Backward

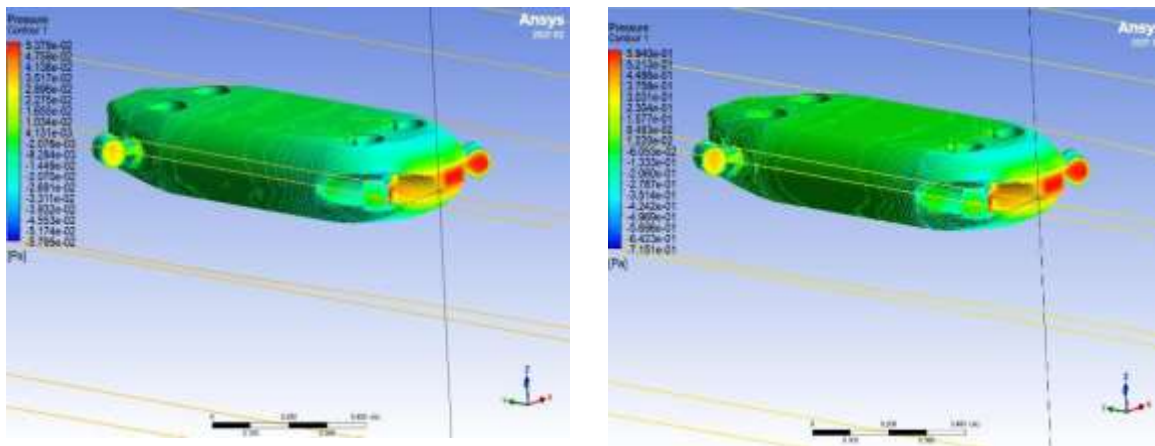


Figure 7 (left: Ship condition at 0.3 m/s), (right: Ship condition at 1.0 m/s)

After conducting resistance tests when the ship goes back and forth, the next is testing the ship's resistance to variations in ship speed when the ship moves to the right and left. The result is that the ship moving to the side makes the resistance greater than the movement of the ship forward and backward, due to several factors, namely the wider surface volume of the ship is one of the causes of greater ship resistance. The resistance of the ship moving sideways from right to left at a speed of 0.3 m/s is 0.004898206 N, and the resistance continues to increase when the speed is added up to 1 m/s with a resistance of 0.048133036 N. These results are not much different when the ship moves in the opposite direction, namely from left to right as shown in Table 5.

Table 5 Result of Resistance of the Ship Moving Sideways from Right to Left

No	Speed (m/s)	Resistance (N)	
		Right – Left	Left - Right
1	0,30	0,004898206	0,004883742
2	0,40	0,008398824	0,008385181
3	0,55	0,015313802	0,015321655
4	0,60	0,018043738	0,018073854
5	0,70	0,024251713	0,024234513
6	1,00	0,048133036	0,047969385

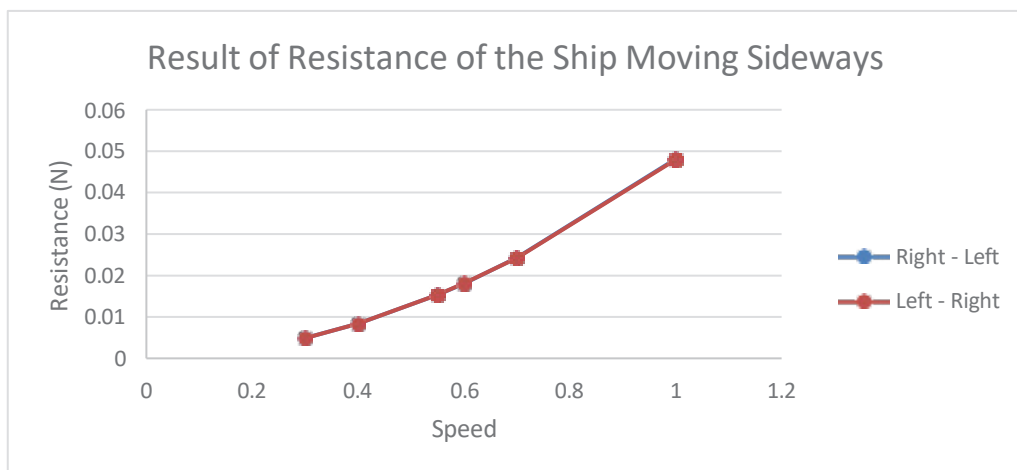


Figure 8 Diagram Result of Resistance of the Ship Moving Sideways from Right to Left.

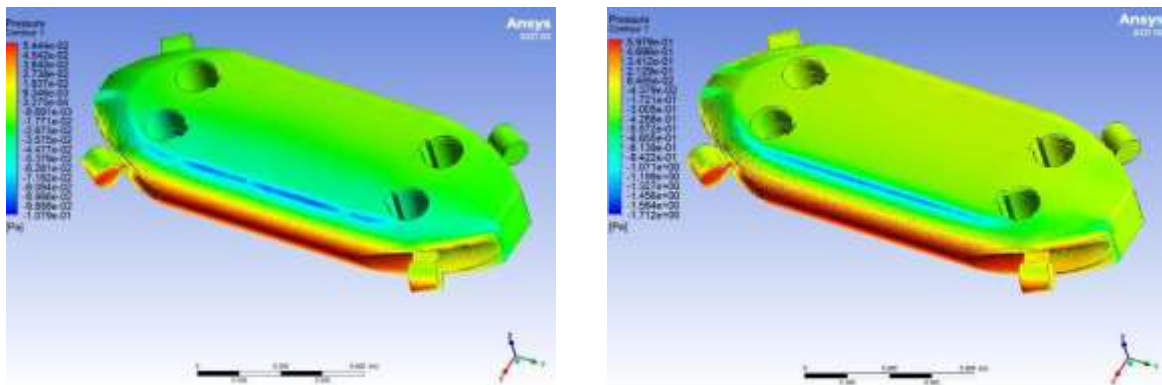


Figure 9 (left: Ship condition at 0.3 m/s), (right: Ship condition at 1.0 m/s)

4. Conclusion

The grid independence tests demonstrated that numerical convergence was achieved when the mesh density was sufficiently refined. Based on the results, the optimal mesh resolution was identified at 1,163,064 elements, where the deviation in ship resistance was minimal, ensuring a balance between computational efficiency and accuracy. In the resistance tests, it was observed that ship resistance increased with speed, consistent with theoretical expectations. For forward and backward movement, resistance ranged from 0.0019 N at 0.3 m/s to 0.0190 N at 1.0 m/s. Additionally, when the ship moved sideways, the resistance was significantly higher due to the increased surface area exposed to the fluid, starting at 0.0049 N at 0.3 m/s and reaching 0.0481 N at 1.0 m/s. The resistance on the ROV increases as the speed of the ROV increases, therefore it is necessary to conduct a study on the service speed of the ROV SN-01 because it can affect the selection of the engine used so that the ROV can work effectively and efficiently. These findings highlight the impact of motion direction and speed on hydrodynamic resistance, providing valuable insights for ship design and operational efficiency. These results can inform future analyses and improvements in maritime engineering.

References

- [1] Aryawan, W.D., Utama, I.K.A.P., Hermawan, Y.A., & Sutiyo 2023. CFD Analysis into the Resistance Characteristics of Remotely Operated Vehicles when Submerges Under Water and Sails on the Surface. *CFD Letters*. 15(8). 166–178.
- [2] ITTC. (2011). Practical Guidelines for Ship CFD Applications. *ITTC – Recommended Procedures and Guidelines ITTC*, 1–8.
- [3] ITTC. (2021a). ITTC-Recommended Procedures and Guidelines Uncertainty Analysis in CFD Verification and Validation Methodology and Procedures ITTC Quality System Manual Recommended Procedures and Guidelines Procedure Uncertainty Analysis in CFD Verification and Validatio. *ITTC - Recommended Procedures and Guidelines*.
- [4] ITTC. (2021b). ITTC - Recommended Procedures and Guidelines: Captive Model Test. *International Towing Tank Conference*, 1–20.
- [5] Ramadhani, K. R. (2023). *Studi dan Rancang Bangun Unmanned Underwater Vehicle (UUV) Untuk Perairan Indonesia*. Institut Teknologi Sepuluh Nopember.
- [6] Sahir, A. A., Munazid, A., & Suwasono, B. (2017). *Perancangan Kapal Selam Tanpa Awak (Unmanned Underwater Vehicle / Uuv) Sebagai Sarana Observasi Bawah Laut*. 72–83.
- [7] Suastika, K 2023 *Dinamika Fluida Komputasi : Metode Volume Hingga* (Surabaya: ITS Press)
- [8] Versteeg, H., & Malalasekera, W 1955 *An Introduction to Computational Fluid Dynamics* (England: Longman Scientific & Technical)